Elsevier Editorial System(tm) for Journal of Catalysis

Manuscript Draft

Manuscript Number:

Title: Photocatalytic hydrogen production from degradation of glucose over fluorinated and platinized TiO2 catalysts.

Article Type: Research Paper

Keywords: Heterogeneous photocatalysis; H2 production; TiO2 surface modification; sugar wastewater.

Corresponding Author: Dr. Vincenzo Vaiano,

Corresponding Author's Institution: University of Salerno

First Author: Giuseppina Iervolino

Order of Authors: Giuseppina Iervolino; Vincenzo Vaiano; Julie J Murcia; Luigi Rizzo; Giovanni Ventre; Giacomo Pepe; Pietro Campiglia; Maria C Hidalgo; Jose A Navio

Dear Editor,

I kindly ask you to consider for possible publication our paper in “Journal of Catalysis”.
The title of our paper is:

Photocatalytic hydrogen production from degradation of glucose over fluorinated and platinized TiO_2 catalysts

The manuscript is an original and novel contribution and relevant to topics of interest for this journal.

This work regards the renewable hydrogen production by photocatalytic degradation of glucose over commercial and home prepared TiO_2 modified by simultaneous fluorine and Pt addition (Pt-F-TiO_2). According to the results achieved in this work, fluorinated TiO_2 (F-TiO_2) represents an interesting support for noble metals to be used in the photocatalytic process for the hydrogen production from sugars contained in water.

At the best of our knowledge, it is the first paper reporting the use of F-TiO_2 as support for noble metals in the photocatalytic production of hydrogen from water polluted by organic compounds.

Sincerely,

The corresponding author.

Vincenzo Vaiano, Ph.D.
Department of Industrial Engineering
University of Salerno,
Via Giovanni Paolo II 132, 84084 Fisciano (Sa), Italy
Phone (089) 964006
Email: vvaiano@unisa.it

*Referee Suggestions

Suggested Reviewers:

Giovanni Palmisano
gpalmisano@masdar.ac.ae

Mohammad Hajaghazadeh
hajaghazadeh@gmail.com

Elisa Isabel Garcia Lopez
elisaisabel.garcialopez@unipa.it

Maria Cristina Paganini
mariacristina.paganini@unito.it

Graphical Abstract (for review)

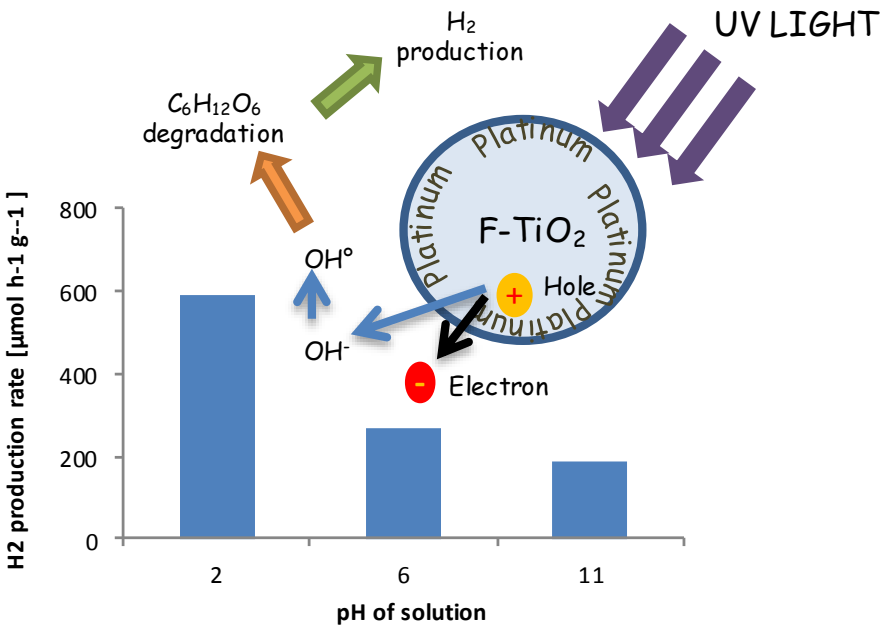

Highlights (for review)

1. Fluorinated TiO_2 as support for Pt in the photocatalytic hydrogen production from glucose.
2. Fluorination and Pt addition modified the hydroxylation of TiO_2 surface.
3. Comparison between sulfation and fluorination of TiO_2 surface.
4. Fluorination of TiO_2 leads to higher glucose degradation rate.
5. The highest photocatalytic activity was obtained on Pt–F–TiO_2 catalysts.

Photocatalytic hydrogen production from degradation of glucose over fluorinated and platinized TiO_2 catalysts

G. Iervolino[1], V. Vaiano[1*], J. J Murcia[3], L. Rizzo[2], G. Ventre[5], G. Pepe[5], P. Campiglia[5], M. C. Hidalgo[4], J. A. Navío[4] and D. Sannino[1]

[1]Department of Industrial Engineering, University of Salerno, via Giovanni Paolo II, 132, 84084 Fisciano (SA) – Italy,

[2] Department of Civil Engineering, University of Salerno, Italy

[3] Grupo de Catálisis, Escuela de Ciencias Químicas, Universidad Pedagógica y Tecnológica de Colombia, Avenida Central del Norte, Tunja, Boyacá – Colombia

[4] Instituto de Ciencia de Materiales de Sevilla (ICMS), Consejo Superior de Investigaciones Científicas (CSIC), Universidad de Sevilla, Américo Vespucio 49, 41092 Sevilla – Spain

[5] Department of Pharmacy, University of Salerno, via Giovanni Paolo II, 132, 84084 Fisciano (SA) – Italy

*vvaiano@unisa.it

Abstract

The present work reports the renewable hydrogen production by photocatalytic degradation of glucose over commercial and home prepared TiO_2 modified by simultaneous fluorine and Pt addition (Pt-F-TiO_2). The obtained materials were widely characterized by different techniques (XRD, S_{BET}, UV-Vis DRS, XRF and TEM) and it was found that surface area, anatase/rutile ratio and the distribution and size of the platinum particles are important

factors influencing the effectiveness of these materials in the H_2 production. The photocatalytic H_2 production from the glucose solution was 97 μmol of H_2 after 3 hours of irradiation on home prepared TiO_2 modified by F and Pt addition, while a lower value corresponding to 31 μmol of H_2 was obtained on commercial TiO_2 modified by F and Pt, after 3 hours of irradiation. The hydrogen production rate increased by decreasing the initial pH of solution reaching the highest value of about 590 μmol $h^{-1}g^{-1}$ after 3 hour of irradiation time at pH=2. Accordingly, sugar containing wastewaters from food industry have the potential for producing hydrogen by photocatalytic process while removing organics before disposal or reuse.

Keywords: Heterogeneous photocatalysis, H_2 production, TiO_2 surface modification, sugar wastewater.

1. Introduction

The demand for hydrogen for both traditional uses (ammonia, methanol and refinery) and running fuel cells is expected to grow over the coming decade [1]. At least in the near future, this hydrogen needs will mainly be satisfied by the reforming of fossil fuels. However, reformed fossil fuels, emitting huge amounts of carbon dioxide, contribute to the increase of greenhouse effect [2]. One approach to limit fossil carbon dioxide emissions while producing H_2 is to apply reforming methods to alternative renewable materials which can be derived from plant crops, agricultural residues, woody biomass, etc. Clean biomass and biomass-derived precursors such as ethanol and sugars are appropriate precursors for producing hydrogen through different conversion strategies [1]. Among sugars, glucose is

one of the most important building blocks in carbohydrate family and also good source for hydrogen production because it has a high hydrogen/carbon ratio and can be easily obtained from renewable biomass such as cellulose and starch [3]. Glucose also occurs in wastewater which should be treated before of their disposal or reuse [4-7].

Glucose can be converted to hydrogen by several reactions such as steam reforming [8], wet oxidation of glucose [9], oxidative glucose reforming [10], dark fermentation [11], electrolysis [12] and photocatalytic oxidation [13]. As alternative, the generation of H_2 by using heterogeneous photocatalysis is a promising route for the production of a sustainable green fuel and, in particular, the photocatalytic hydrogen production from biomass glucose decomposition seems to offer a very powerful method among the practical and low-cost technologies in the hydrogen–based energy system [14]. It is well known that the photocatalytic reactions take place when the semiconductor particle absorbs a photon of light which is more energetic than its band gap. Thus an electron is excited from the valence band to the conduction band, leaving a hole at the valence band. In aqueous solutions the hole may be trapped by H_2O or OH^- adsorbed at the surface, thus forming the highly reactive hydroxyl radical, which can promote the oxidation of organic compounds [15-18]. The mechanism of these reactions has been intensively studied and TiO_2 is one of the most investigated semiconductors for photocatalytic applications [19, 20].

The properties of TiO_2 such as surface area, surface charge, crystallinity, particle size and lattice defects affect photocatalytic activities in a complex way. The surface of TiO_2 is particularly important in determining the photocatalytic reaction kinetics, mechanisms, and efficiencies because the photocatalytic reactions mostly take place on the surface of the

TiO_2 [21]. Surface modifications of semiconductor photocatalysts may have a marked influence on the photocatalytic processes occurring at the water-semiconductor interface [22]. With respect to commercial titania samples, TiO_2 modified with fluorine (F-TiO_2) inhibits the recombination rate of holes and free electrons, enhancing the photocatalytic activity [23]

In particular, it has been reported that F-TiO_2 is an effective material in the photocatalytic removal of not biodegradable contaminants (such as phenol or methylene blue) [4, 23-25].

Despite Pt/TiO_2 photocatalysts were studied for the hydrogen production by photocatalytic reforming of organic substance such as methanol [26], no article reports the use of F-TiO_2 as support for noble metals in the photocatalytic production of hydrogen from water polluted by organic compounds. For this reason, in the present work, platinized F-TiO_2 photocatalysts were studied with the aim to produce hydrogen from the degradation of glucose. The effect of the TiO_2 source, the TiO_2 fluorination, the presence of Pt nanoparticles and the initial pH of the reaction solution over the hydrogen evolution and glucose degradation were investigated.

2. Experimental

2.1 Photocatalysts preparation

TiO_2 was prepared by hydrolysis of titanium tetraisopropoxide in isopropanol solution by the slow addition of distilled water (volume ratio isopropanol/water 1:1).The powder was recovered by filtration and dried at 110ºC overnight. A fraction of this material was calcined at 650 °C for 2 h and the sample thus obtained was called home prepared TiO_2 (hp-TiO_2). Commercial TiO_2 Evonik P25 was used as received.

Fluorinated samples were prepared by adding 10 mM NaF to an aqueous suspension of uncalcined hp-TiO_2 or P25, these materials were named F-TiO_2 and F-P25, respectively. In order to maximize fluoride adsorption, the pH was adjusted to 3 using 1 M HCl solution [25]. This suspension was stirred for 1 hour in the dark. In order to compare the effect of the TiO_2 modification by fluorination or sulfation, a hp-TiO_2 was immersed in a 1M H_2SO_4 solution and stirred for 1h. Precipitate of fluorinated or sulfated TiO_2 (S-TiO_2) was recovered by filtration, dried and calcined at 650 °C for 2 h.

Platinum was deposited on the surface of the fluorinated or sulfated samples by photodeposition method, using hexachloroplatinic acid (H_2PtCl_6, Aldrich 99.9%) as metal precursor. The final amount of Pt was 0.5 wt%. A suspension of the corresponding F-TiO_2, F-P25 or S-TiO_2 sample in distilled water containing isopropanol (Merck 99.8%) and the appropriate amount of H_2PtCl_6 used as precursor for Pt nanoparticles was prepared. Pt photodeposition was then performed under an inert atmosphere (N_2), by illuminating the suspension for 120 min with an Osram Ultra-Vitalux lamp (300 W) which possesses a sun-like radiation spectrum with a main emission line in the UVA range at 365 nm. Light intensity on the suspensions, used for the photodeposition of platinum, was 60 W/m^2 [27]. After photodeposition, the powders were recovered by filtration and dried at 110ºC overnight. All the prepared photocatalysts are reported in Table 1.

2.2 Photocatalysts characterization

X-ray diffraction (XRD) was performed using a Siemens D-501 diffractometer with Ni filter and graphite monochromator using Cu Kα radiation. Crystallite size was estimated

from the line broadening of the main X-ray diffraction peaks by using the Scherrer equation. Peaks were fitted by using a Voigt function.

Surface area (S_{BET}) was determined by using the Brunauer–Emmett–Teller method, and this analysis was carried out by N_2 adsorption at 77 K using a Micromeritics ASAP 2010 instrument.

Light absorption properties of the samples were studied by UV–Vis spectrophotometry using a Varian Cary 100 UV–Vis spectrophotometer coupled to an integration sphere for diffuse reflectance studies. $BaSO_4$ was used as reference. Band gaps values were calculated from the corresponding Kubelka–Munk functions ($F(R\infty)$), which are proportional to the absorption of radiation, by plotting $(F(R\infty) \times h\nu)^{1/2}$ against $h\nu$ [28].

Chemical composition of the samples was determined by X-ray fluorescence spectrometry (XRF) in a Panalytical Axios sequential spectrometer equipped with a rhodium tube as the source of radiation. XRF measurements were performed onto pressed pellets (sample included in 10 wt.% of wax).

Platinum particle sizes were studied by TEM in a Philips CM 200 microscope. The samples were dispersed in ethanol using an ultrasonicator and dropped on a carbon grid, Determination of the metal particle average diameter ($\bar{d}$) in the different samples was accomplished by counting particles in a high number of TEM images from different places of the samples. The following equation was used: ($\bar{d}$nm)=Σ *di x fi*

where *di* is the diameter of the *ni* counted particles and *fi* is the particle size distribution estimated by:

$$fi = \frac{ni}{\sum ni}$$

Where *ni* is the number of particles of diameter *di*.

X-ray photoelectron spectroscopy (XPS) studies were carried out on a Leybold–Heraeus LHS-10 spectrometer, working with constant pass energy of 50 eV. The spectrometer main chamber, working at a pressure $<2\times10^{-9}$ Torr, is equipped with an EA-200 MCD hemispherical electron analyzer with a dual X-ray source working with Al Kα (hν = 1486.6 eV) at 120 W and 30 mA. C 1s signal (284.6 eV) was used as internal energy reference in all the experiments.

2.3 Photocatalytic experiments

Photocatalytic experiments were carried out in a pyrex cylindrical reactor (ID = 2.5 cm) equipped with an N_2 distributor device (Q=0.122 NL/min). The continuous mixing of glucose solution and the photocatalyst was realized by external recirculation of water through the use of a peristaltic pump. The photoreactor was irradiated by a UV-LEDs strip (nominal power: 10W) with wavelength emission in the range 375–380 nm. LEDs strip was positioned around and in contact with the external surface of the reactor to make reaction volume uniformly irradiated by the light source.

In a typical photocatalytic test, 0.12 g of catalyst was suspended in 80 ml aqueous solution containing 2000 mg/L of glucose (D + Glucose VWR, Sigma Aldrich). The suspension was left in dark condition for 2 hours to reach the adsorption-desorption equilibrium of glucose

on the photocatalysts surface, and then photocatalytic reaction was initiated under UV light up to 3 hours.

In order to evaluate the influence of the initial pH of the solution on the production of H_2 and CO_2, the pH of solution was adjusted by adding nitric acid (Baker Analyzed, 65%) or Ammonium Hydroxide (Baker Analyzed, 30%). About 2 mL of samples were taken from the photoreactor at different times and filtered in order to remove catalyst particles before analysis.

Hydrogen yield was evaluated according to the following relationship [7]

$$R_{H_2} = \frac{2 \cdot nH_2}{12 \cdot n^0 C_6 H_{12} O_6} \cdot 100$$

Where:

RH_2=hydrogen yield;

nH_2=moles of H_2 produced during the irradiation;

$n^0C_6H_{12}O_6$ = moles of glucose after dark adsorption.

The quantum efficiency (QE) of photocatalysts was calculated according to the following equation [29]:

$$QE[\%] = \frac{N_{H_2} \cdot 2}{N_{photons}} \cdot 100$$

Where:

N_{H2}= number of evolved H_2 molecules per second;

$N_{photons}$= number of incident photons per second.

The number of incident photons on the external surface of the photoreactor was $2.014x10^{16}$ photons/s, measured by using a LMV UV-Meter.

2.4 Analytical measurement

The analysis of the gaseous phase coming from the photoreactor was performed by using continuous analyzers (ABB Advance Optima) to measure the concentration of CO, CO_2, O_2, CH_4 and H_2.

For the evaluation of the concentration of glucose and arabinose in liquid phase, was employed by high-performance liquid chromatography (HPLC) using a Shimadzu Nexera LC-30A system (Shimadzu, Kyoto, Japan), consisting of a controller CBM-20A, two dual-plunger parallel-flow pumps LC-30AD, a degasser DGU-20 A5R, an autosampler SIL-30 AC, a column oven CTO-20AC and a evaporative light scattering (ELSD) detector. Mobile phase used was composed by H_2O (A) and CH_3CN (B), the following binary gradient was applied: 0.01-4.50 min, 74-80% B; 4.50-4.51 min, 80-74% B; 4.51-8.00 min, isocratic at 74% B. Flow rate was set to 0.80 mL/min. The oven temperature was set at 25 °C. The injection volume of the sample analyzed was 5 µL. The chromatogram was monitored by ELSD with the following parameters (Gain 5, T = 70 °C, N2 = 270KPa). For the separation, an Supelcosil LC-NH2 150 mm × 3 mm × 3 µm (L × ID × particle size, 120 Å) was employed (Supelco, Belle-fonte, PA, USA). The data were processed by the LabSolutions® software (Version 3.50.346, Shimadzu). The gluconic acid formed during the irradiation time was analyzed by the UV absorption of liquid samples at 264 nm [30] using UV-Vis spectrophotometer (Lambda 35, Perkin Elmer).

3. Results and discussion

3.1 Photocatalysts characterization results

3.1.1. X-ray diffraction (XRD)

XRD analysis showed that hp-TiO_2 and P25 samples contain rutile and anatase phases (Figure 1); the anatase to rutile ratio for these samples was 90:10 and 80:20, respectively. XRD analysis also showed that only anatase phase results from fluorination process in F-TiO_2 (home prepared sample) catalyst, according to previous works that had documented how fluorination inhibits the formation of rutile phase of TiO_2 during the calcination process [25, 31]. In the case of P25, after fluorination and calcination, anatase:rutile ratio is almost the same. The anatase crystallite size ($D_{anatase}$) calculated by the Scherrer equation from the (1 0 1) peak of the XRD pattern are listed in Table 1. As observed, hp-TiO_2 presents the lowest value and after fluorination this value notably increases. This result is in agreement with previous studies where it was observed that fluoride enhanced the crystallization of anatase phase and promoted the growth of crystallites [32, 33].

3.1.2 BET Surface Area

BET surface area values (S_{BET}) for all samples are shown in Table 1. Hp-TiO_2 presents the lowest specific surface area (11 m^2/g); this can be due to the large degree of particles sintering during the calcination process [25]. As it can be observed the S_{BET} of hp-TiO_2 considerably increases after fluorination or sulfation; in fact these ions protect anatase phase against rutilization and sintering, preserving the surface area during the calcination process [25]. The fluorination of P25 did not induce significant modification on this

parameter. It was also observed that Pt addition induces a slight decrease in the S_{BET} value; this is probably due to pore blocking by metal deposits on the modified TiO_2 surface.

3.1.3 UV-Vis Diffuse Reflectance spectra

The light absorption properties of the photocatalysts were evaluated by UV-Vis DRS analysis (Figure 2), and it was observed a slight increase of the absorption throughout the visible range of the spectrum in the fluorinated and platinized samples; this is mainly due to the grey color of these materials. In the platinized catalysts (inset in Figure 2), three small peaks located at ca. 450, 520 and 700 nm were observed; these peaks can be attributed to the Pt clusters and also with the visible-light-induced electron transfer from the metal nanoparticles to the TiO_2 particle [34]. Surface plasmon resonance of Pt nanoparticles excited by visible light facilitates the excitation of the surface electron and promotes interfacial electron transfer process, thus improving the TiO_2 photoactivity.

The band gap values calculated for the samples are presented in Table 1, as it can be observed this parameter does not significantly modified by the different treatments applied to TiO_2.

3.1.4 X-ray fluorescence

Chemical composition of the samples was evaluated by XRF and it was observed that the real platinum content was 0.36 and 0.39 % for Pt-F-P25 and Pt-F-TiO_2, respectively. These values are under the nominal metal content (0.5 wt%) thus indicating an incomplete reduction of the metal precursor during the synthesis. A negligible amount of Cl^- species,

remained on the platinized solids after preparation, was detected (i.e <0.02 wt %). F or Na species were not detected by XRF.

3.1.5 Microscopic analysis

Platinum particles size was evaluated by TEM and selected micrographs for platinized samples are presented in Figure 3**.** As it can be seen, in the Pt-S-TiO_2 and Pt-F-TiO_2 samples, the Pt nanoparticles (small black dots) are homogeneously distributed on TiO_2 surface. It is worthwhile noting that Pt-F-TiO_2 sample is the only catalyst having Pt nanoparticles in the range 1-2 nm. Moreover, aggregation of Pt particles heterogeneously distributed on titania surface was clearly observed in the Pt-F-P25 sample (Figure 3c). The Pt particle size distribution (*fi*) is also presented in Figure 3. As it can be observed the highest particle size was obtained in the Pt-F-P25 sample (i.e 9-10 nm), it can be due to the presence of the rutile phase in this catalyst which can difficult the homogeneous photodeposition of the metal particles on the titania surface. The best Pt particles dispersion was observed in the catalyst Pt-S-TiO_2 (Figure 3a), in this sample the particles are more homogeneously distributed on surface with sizes between 4-5 nm.

3.1.6 X-ray photoelectron spectroscopy (XPS)

XPS measurements for all the samples were also performed and the obtained spectra are showed in Figure 4. In the O 1s region, a peak located at binding energy of 529.6 ± 0.2 eV was detected for all the samples, corresponding to O^{2-} in the TiO_2 network. In addition, broad shoulder at higher binding energies (530.3 eV) ascribed to oxygen in surface hydroxyl groups were also observed. On the other hand, the Ti 2p core level spectra were

similar for all the studied samples with peaks of binding energies located at 458 ± 0.5 eV, ascribed to Ti^{4+} as the main component.

By XPS analyzes it was also detected the presence of Na and fluoride species on the surface fluorinated samples, indicating that ≡Ti-OH_2 species could be substituted by ≡Ti-F [25, 35].

3.2 Photocatalytic activity results

3.2.1 Hydrogen production and glucose degradation under UV-LEDs irradiation for the different fluorinated photocatalysts

Figure 5a and 5b show respectively, the relative glucose concentration (C/C_0) and hydrogen production during the exposition to UV-LEDs irradiation at the spontaneous pH of solution (pH=6) for all the photocatalysts. As expected, no H_2 production was observed in the absence of Pt. On the contrary, the photocatalytic H_2 production from the glucose solution can be significantly enhanced in presence of Pt on TiO_2 surface. In particular, the highest glucose degradation and H_2 production was achieved on Pt-F-TiO_2 catalyst (about 100 µmol after 3 hours of irradiation). This can be due to the presence of the platinum and to its lower particle size distribution and better dispersion of the metal nanoparticles over the anatase surface of F-TiO_2 photocatalyst with respect to F-P25 photocatalyst. Moreover, Pt-F-TiO_2 was also found to be the best photocatalyst for glucose degradation (74% removal after 3 hours of irradiation). For Pt-F-P25 and Pt-F-TiO_2, the only detected byproduct was CO_2 (4.4 µmol).

In Table 2, the H_2 evolution rate and QE values over Pt-F-TiO_2 and Pt-F-P25 catalysts are given. For Pt-F-P25 the H_2 formation rate is estimated to be 0.1 mmol h^{-1}, corresponding to

a QE of 17%. Both values are remarkably increased for Pt-F-TiO_2, reaching values equal to 0.3 mmol h^{-1} and 56 % for H_2 evolution rate and QE, respectively.

3.2.2 Comparison between the photocatalytic activity of Fluorinated and Sulfated platinized TiO_2

Home prepared sulfated titania (Pt-S-TiO_2) performances in terms of glucose degradation (Figure 6a) and H_2 production (Figure 6b) containing the same nominal weight of platinum (0.5 wt%) were compared with home prepared Pt-F-TiO_2. After 3 hours of UV irradiation, the degradation of glucose on Pt-S-TiO_2 (Figure 6a) is equal to 57 % and the H_2 production (Figure 6b) is equal to 82 µmol (H_2 yield of 2%), lower than that obtained with fluorinated titania (glucose degradation and H_2 yield equal to 74% and 4%, respectively). These results are in agreement with scientific literature regarding photocatalytic activity of F-TiO_2 in both the removal of pollutants from wastewater and hydrogen production [36]. Accordingly, the increase of photocatalytic activity of the fluorinated sample is due to the formation of unbounded •OH that are more reactive than •OH trapped on catalyst surface [37, 38]. These results also can be related to the higher absorption of the fluorinated sample in the visible region as it can be observed in Figure 2.

3.2.3 Effect of initial pH

Due to higher performances of Pt-F-TiO_2, this catalyst was chosen to evaluate the effect of initial pH over both the degradation of glucose and the production of hydrogen (Figure 7). The degradation of glucose is higher at pH=6, reaching a value equal to 73% (Figure 7a)

while the best hydrogen evolution rate was obtained at pH=2 (Figure 7b). It has been reported that, in acidic conditions, the redox potential of H^+/H_2 would become more positive, and this condition is advantageous for an efficient hydrogen photocatalytic generation [5]. In our previous work, H_2 production from glucose solutions on sulfated Pd-TiO_2 photocatalysts was investigated [7]. Accordingly, the higher hydrogen yield was obtained in acidic condition (3 % after 3 hours of irradiation; H_2 production: 590 μmol h^{-1} g^{-1}). However, at pH=2, when the glucose in the solution is mainly in molecular form [5], the degradation of glucose occurs in limited extent.

3.2.4 Possible reaction mechanism

In this work it was also proposed a possible reaction mechanism for the photocatalytic hydrogen production from glucose aqueous solution. Usually, in the literature, the mechanism for the H_2 production is explained according to the classical reaction of glucose photoreforming [39]:

$$C_6H_{12}O_6(l) + 6\ H_2O(l) = 6\ CO_2(g) + 12\ H_2(l) \qquad \text{Eq. 1}$$

In this reaction the H_2/CO_2 ratio is equal to 2. However, in our case, this ratio is never equal to 2, but it is in the range between 10 and 30, as it is possible to evince from experimental data reported in Figure 5. This indicates that the mechanism of production of H_2 from glucose does not take place according to the Eq.1. Moreover, from HPLC results, no formation of intermediate compounds resulting from the glucose conversion, such as arabinose [30], was observed during the irradiation. In fact, in the HPLC chromatogram obtained after 3 hours of UV irradiation, only the signal related to glucose was visible, with a peak that decreased with respect to the initial solution (Figure 8). It is possible to

highlight that there was not the presence of arabinose, which should appear in a different retention time from glucose (Figure 9).

Gluconic acid ($C_6H_{12}O_7$), a typical glucose oxidation intermediate, was the sole intermediate detected in the solution after 3 hours of UV irradiation by UV Vis spectrophotometric analysis.

This last result therefore suggests that, in agreement with the literature results [30], a possible reaction mechanism for the photocatalytic H_2 production from glucose on Pt-F-TiO_2, providing the presence of gluconic acid in solution, is the following:

$h^+ + H_2O = \bullet OH + H^+$ Eq. 2

$h^+ + OH^- = \bullet OH$ Eq. 3

$H^+ + e^- = ½\ H_2$ (on Pt) Eq. 4

$RCHO + \bullet OH = RCO\bullet + H_2O$ Eq. 5

or

$h^+ + RCHO = RCO\bullet + H^+$ Eq. 6

$RCO\bullet + H_2O = RCOOH + \bullet H$ Eq. 7

$RCOOH + \bullet OH = R'OH\ (R''CHO) + CO_2 + \bullet H$ Eq. 8

$2e^- + 2H^+ = \bullet H + \bullet H$ Eq. 9

$\bullet H + \bullet H = H_2$ Eq. 10

Where :

$RCHO = C_6H_{12}O_6$

$RCOOH = C_6H_{12}O_7$

The reaction is initiated by the photoexcitation of Pt-F-TiO_2 photocatalyst, leading to the formation of electron–hole pairs. Valence band holes (h^+) can be filled by the surface water

molecules or hydroxyl ions to form hydroxyl radicals (Eqs. 2-3) [30].Pt can trap photogenerated conduction electron (e^-), and consequently the electron acceptor (H^+) interacts with the electron to produce hydrogen on Pt (Eq. 4) [40].Glucose (RCHO) adsorbed on the catalyst can react with the hydroxyl radicals (Eq. 5) forming gluconic acid (Eq. 7) which would react further with hydroxyl radicals so that a decarboxylation reaction takes place (Eq. 8) [20]. The holes could react also directly with electron donor glucose (Eq. 6). The produced •H radicals can form H_2 (Eq. 9-10) [30]. The amount of CO_2 was found higher on Pt-F-TiO_2 than on Pt-S-TiO_2, indicating a certain relevance of (Eq. 8) on the photocatalytic activity.

4. Conclusion

Glucose, typically occurring in some food industry wastewater, looks an interesting source for hydrogen production by photocatalytic treatment because of its high hydrogen/carbon ratio. According to the results achieved in this work, fluorinated TiO_2 (F-TiO_2) represents an interesting support for noble metals to be used in the photocatalytic process for the hydrogen production sugars contained in water. In particular, Pt on F-TiO_2 (Pt-F-TiO_2) significantly enhanced the photocatalytic H_2 production compared to the other investigated catalysts. The increase of photocatalytic activity of Pt-F-TiO_2, with respect to Pt supported on sulfated TiO_2, is due to the formation of unbounded OH radicals that are more reactive, leading to a higher hydrogen production.

Furthermore the higher hydrogen production was obtained under acidic conditions (pH=2), while the degradation of glucose was higher at pH=6. It was also confirmed, by HPLC and UV-vis analyzes performed on the liquid samples, that using Pt-F-TiO_2, it is possible to

produce hydrogen by the photocatalytic degradation of glucose obtaining gluconic acid as product.

Acknowledgements

CITIUS (University of Seville) is acknowledged for XPS and XRF measurements. Universidad Pedagógica y Tecnológica de Colombia is acknowledged for the financial support. Diana Sannino wishes to thank the financial support of University of Salerno through "Fondi di Ateneo per la Ricerca di Base (FARB)".

References

[1] R.M. Navarro, M.C. Sánchez-Sánchez, M.C. Alvarez-Galvan, F.D. Valle, J.L.G. Fierro, Hydrogen production from renewable sources: Biomass and photocatalytic opportunities, Energy and Environmental Science, 2 (2009) 35-54.
[2] D.L. Trimm, Z.I. Önsan, Onboard Fuel Conversion for Hydrogen-Fuel-Cell-Driven Vehicles, Catalysis Reviews - Science and Engineering, 43 (2001) 30-84.
[3] A.M. Ruppert, K. Weinberg, R. Palkovits, Hydrogenolysis goes bio: From carbohydrates and sugar alcohols to platform chemicals, Angewandte Chemie - International Edition, 51 (2012) 2564-2601.
[4] X. Fu, J. Long, X. Wang, D.Y.C. Leung, Z. Ding, L. Wu, Z. Zhang, Z. Li, X. Fu, Photocatalytic reforming of biomass: A systematic study of hydrogen evolution from glucose solution, International Journal of Hydrogen Energy, 33 (2008) 6484-6491.
[5] D. Jing, M. Liu, J. Shi, W. Tang, L. Guo, Hydrogen production under visible light by photocatalytic reforming of glucose over an oxide solid solution photocatalyst, Catalysis Communications, 12 (2010) 264-267.
[6] G. Iervolino, V. Vaiano, D. Sannino, L. Rizzo, P. Ciambelli, Production of hydrogen from glucose by LaFeO3 based photocatalytic process during water treatment, International Journal of Hydrogen Energy, 41 (2016) 959-966.
[7] V. Vaiano, G. Iervolino, G. Sarno, D. Sannino, L. Rizzo, J.J. Murcia Mesa, M.C. Hidalgo, J.A. Navío, Simultaneous production of CH4 and H2 from photocatalytic reforming of glucose aqueous solution on sulfated Pd-TiO2 catalysts, Oil and Gas Science and Technology, 70 (2015) 891-902.
[8] O. Bičáková, P. Straka, Production of hydrogen from renewable resources and its effectiveness, International Journal of Hydrogen Energy, 37 (2012) 11563-11578.

[9] T. Moreno, G. Kouzaki, M. Sasaki, M. Goto, M.J. Cocero, Uncatalysed wet oxidation of d-glucose with hydrogen peroxide and its combination with hydrothermal electrolysis, Carbohydrate Research, 349 (2012) 33-38.
[10] U. Prüße, M. Herrmann, C. Baatz, N. Decker, Gold-catalyzed selective glucose oxidation at high glucose concentrations and oxygen partial pressures, Applied Catalysis A: General, 406 (2011) 89-93.
[11] D. Ghosh, P.C. Hallenbeck, Fermentative hydrogen yields from different sugars by batch cultures of metabolically engineered Escherichia coli DJT135, International Journal of Hydrogen Energy, 34 (2009) 7979-7982.
[12] J. McGinley, F.N. McHale, P. Hughes, C.N. Reid, A.P. McHale, Production of electrical energy from carbohydrates using a transition metal-catalysed liquid alkaline fuel cell, Biotechnology Letters, 26 (2004) 1771-1776.
[13] H. Bahruji, M. Bowker, P.R. Davies, L.S. Al-Mazroai, A. Dickinson, J. Greaves, D. James, L. Millard, F. Pedrono, Sustainable H2 gas production by photocatalysis, J. Photochem. Photobiol., A, 216 (2010) 115-118.
[14] X. Fu, J. Long, X. Wang, D.Y.C. Leung, Z. Ding, L. Wu, Z. Zhang, Z. Li, X. Fu, Photocatalytic reforming of biomass: A systematic study of hydrogen evolution from glucose solution, Int. J. Hydrogen Energy, 33 (2008) 6484-6491.
[15] V. Vaiano, O. Sacco, G. Iervolino, D. Sannino, P. Ciambelli, R. Liguori, E. Bezzeccheri, A. Rubino, Enhanced visible light photocatalytic activity by up-conversion phosphors modified N-doped TiO<inf>2</inf>, Applied Catalysis B: Environmental, 176-177 (2015) 594-600.
[16] V. Vaiano, O. Sacco, D. Sannino, P. Ciambelli, S. Longo, V. Venditto, G. Guerra, N-doped TiO2/s-PS aerogels for photocatalytic degradation of organic dyes in wastewater under visible light irradiation, Journal of Chemical Technology and Biotechnology, 89 (2014) 1175-1181.
[17] D. Sannino, V. Vaiano, P. Ciambelli, P. Eloy, E.M. Gaigneaux, Avoiding the deactivation of sulphated MoO x/TiO 2 catalysts in the photocatalytic cyclohexane oxidative dehydrogenation by a fluidized bed photoreactor, Applied Catalysis A: General, 394 (2011) 71-78.
[18] P. Ciambelli, D. Sannino, V. Palma, V. Vaiano, Cyclohexane photocatalytic oxidative dehydrogenation to benzene on sulphated titania supported MoOx, in: Studies in Surface Science and Catalysis, 2005, pp. 179-187.
[19] Q.H. Zhang, L. Gao, J.K. Guo, Photo catalytic activity of nanosized TiO2, Wuji Cailiao Xuebao/Journal of Inorganic Materials, 15 (2000) 560.
[20] M.R. Hoffmann, S.T. Martin, W. Choi, D.W. Bahnemann, Environmental applications of semiconductor photocatalysis, Chemical Reviews, 95 (1995) 69-96.
[21] J. Kim, W. Choi, TiO2 modified with both phosphate and platinum and its photocatalytic activities, Applied Catalysis B: Environmental, 106 (2011) 39-45.
[22] S.y. Yang, Y.y. Chen, J.g. Zheng, Y.j. Cui, Enhanced photocatalytic activity of TiO2 by surface fluorination in degradation of organic cationic compound, Journal of Environmental Sciences, 19 (2007) 86-89.
[23] Y.N. Tan, C.L. Wong, A.R. Mohamed, Hydrothermal treatment of fluorinated titanium dioxide: Photocatalytic degradation of phenol, Asia-Pacific Journal of Chemical Engineering, 7 (2012) 877-885.

[24] C. Yu, J.C. Yu, M. Chan, Sonochemical fabrication of fluorinated mesoporous titanium dioxide microspheres, Journal of Solid State Chemistry, 182 (2009) 1061-1069.
[25] J.J. Murcia, M.C. Hidalgo, J.A. Navío, J. Araña, J.M. Doña-Rodríguez, Study of the phenol photocatalytic degradation over TiO<inf>2</inf> modified by sulfation, fluorination, and platinum nanoparticles photodeposition, Applied Catalysis B: Environmental, 179 (2015) 305-312.
[26] G.N. Nomikos, P. Panagiotopoulou, D.I. Kondarides, X.E. Verykios, Kinetic and mechanistic study of the photocatalytic reforming of methanol over Pt/TiO2 catalyst, Applied Catalysis B: Environmental, 146 (2014) 249-257.
[27] J.J. Murcia, J.A. Navío, M.C. Hidalgo, Insights towards the influence of Pt features on the photocatalytic activity improvement of TiO 2 by platinisation, Applied Catalysis B: Environmental, 126 (2012) 76-85.
[28] S.P. Tandon, J.P. Gupta, MEASUREMENT OF FORBIDDEN ENERGY GAP OF SEMICONDUCTORS BY DIFFUSE REFLECTANCE TECHNIQUE, Phys Status Solidi, 38 (1970) 363-367.
[29] H. Yan, J. Yang, G. Ma, G. Wu, X. Zong, Z. Lei, J. Shi, C. Li, Visible-light-driven hydrogen production with extremely high quantum efficiency on Pt-PdS/CdS photocatalyst, Journal of Catalysis, 266 (2009) 165-168.
[30] Y. Li, J. Wang, S. Peng, G. Lu, S. Li, Photocatalytic hydrogen generation in the presence of glucose over ZnS-coated ZnIn2S4 under visible light irradiation, International Journal of Hydrogen Energy, 35 (2010) 7116-7126.
[31] C. Trapalis, N. Todorova, T. Giannakopoulou, G. Romanos, T. Vaimakis, J. Yu, Preparation of fluorine-doped TiO2 photocatalysts with controlled crystalline structure, International Journal of Photoenergy, 2008 (2008).
[32] J. Yu, Q. Xiang, J. Ran, S. Mann, One-step hydrothermal fabrication and photocatalytic activity of surface-fluorinated TiO2 hollow microspheres and tabular anatase single micro-crystals with high-energy facets, CrystEngComm, 12 (2010) 872-879.
[33] S. Yamabi, H. Imai, Crystal phase control for titanium dioxide films by direct deposition in aqueous solutions, Chemistry of Materials, 14 (2002) 609-614.
[34] M. Maicu, M.C. Hidalgo, G. Colón, J.A. Navío, Comparative study of the photodeposition of Pt, Au and Pd on pre-sulphated TiO2 for the photocatalytic decomposition of phenol, Journal of Photochemistry and Photobiology A: Chemistry, 217 (2011) 275-283.
[35] M.S. Vohra, S. Kim, W. Choi, Effects of surface fluorination of TiO2 on the photocatalytic degradation of tetramethylammonium, Journal of Photochemistry and Photobiology A: Chemistry, 160 (2003) 55-60.
[36] J. Kim, J. Lee, W. Choi, Synergic effect of simultaneous fluorination and platinization of TiO 2 surface on anoxic photocatalytic degradation of organic compounds, Chemical Communications, (2008) 756-758.
[37] H. Park, Y. Park, W. Kim, W. Choi, Surface modification of TiO2 photocatalyst for environmental applications, Journal of Photochemistry and Photobiology C: Photochemistry Reviews, 15 (2013) 1-20.
[38] J. Yu, W. Wang, B. Cheng, B.L. Su, Enhancement of photocatalytic activity of Mesporous TiO2 powders by hydrothermal surface fluorination treatment, Journal of Physical Chemistry C, 113 (2009) 6743-6750.

[39] X. Fu, X. Wang, D.Y.C. Leung, W. Xue, Z. Ding, H. Huang, X. Fu, Photocatalytic reforming of glucose over la doped alkali tantalate photocatalysts for H2 production, Catalysis Communications, 12 (2010) 184-187.
[40] X. Chen, S. Shen, L. Guo, S.S. Mao, Semiconductor-based photocatalytic hydrogen generation, Chemical Reviews, 110 (2010) 6503-6570.

Figures captions

Figure 1. XRD patterns for home prepared and commercial TiO_2 modified by simultaneous fluorination and Pt photodeposition.

Figure 2. UV-Vis DR spectra for the photocatalysts analyzed.

Figure 3. TEM images for analyzed samples. (a) Pt-S-TiO_2, (b) Pt-F-TiO_2 and (c) Pt-F-P25.

Figure 4. XPS core level spectra of O 1s and F 1s regions for selected samples

Figure 5. Behavior of glucose normalized concentration (a) H_2 (b) and CO_2 (c) production as a function of irradiation time; catalyst dose: 1.5 g/L; initial glucose concentration: 2000 mg/L; pH=6.

Figure 6. Behavior of glucose normalized concentration (a) and H_2 rate (b) during irradiation of fluorinated and sulfated TiO_2; catalyst dose: 1.5 g/L; initial glucose concentration: 2000 mg/L; pH=6.

Figure 7. Effect of initial pH on glucose degradation (a) and H_2 production rate (b) for Pt-F-TiO_2 after 3 hours of irradiation; catalysts dose: 1.5 g/L; initial glucose concentration: 2000 mg/L.

Figure 8. Typical HPLC chromatogram obtained during photocatalytic test on Pt-F-TiO_2 catalyst; initial glucose concentration : 2000 mg/L; initial pH =2.

Figure 9. Typical HPLC chromatogram for a standard solution of arabinose.

Tables

Table 1. Summary of the characterization results.

Photocatalyst	**$D_{Anatase}$ (nm)**	**S_{BET} (m^2/g)**	**Band gap (eV)**
P25	22	51	3.23
F-P25	23	50	3.20
Pt-F-P25	21	47	3.20
Hp-TiO_2	17	11	3.30
F-TiO_2	24	51	3.21
Pt-F-TiO_2	23	42	3.24
S-TiO_2	20	58	3.20
Pt-S-TiO_2	20	49	3.17

Table 2. Photocatalytic H_2 evolution rate and QE values for Pt-F-TiO2 and Pt-F-P25 catalysts.

Photocatalyst	**H_2 evolution rate (mmol/h)**	**QE (%)**
Pt-F-P25	0.1	17
Pt-F-TiO_2	0.3	55

Figures

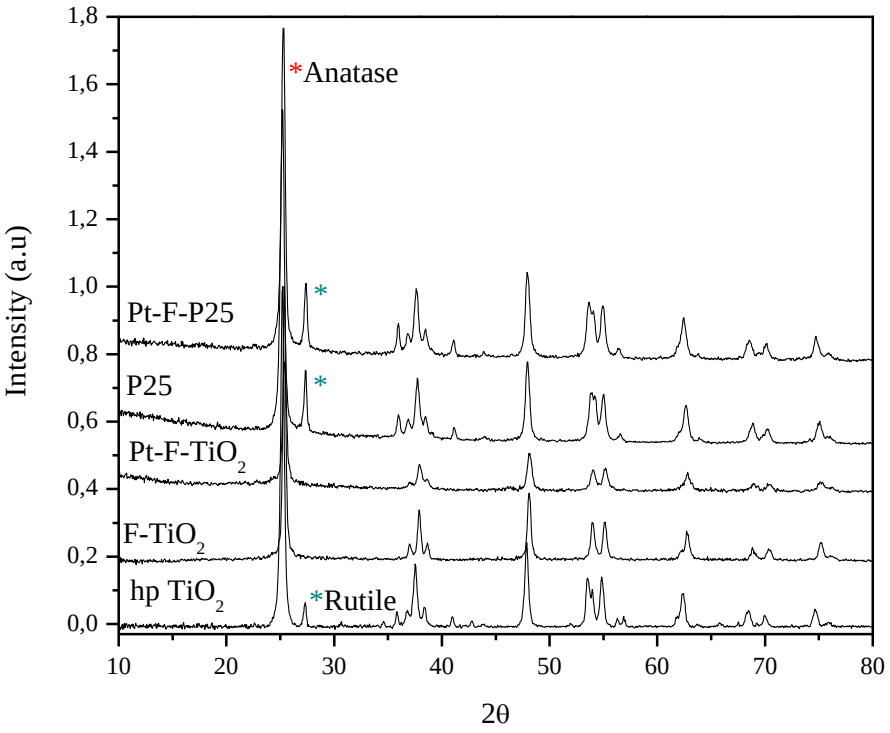

Figure 1. XRD patterns for home prepared and commercial TiO_2 modified by simultaneous fluorination and Pt photodeposition.

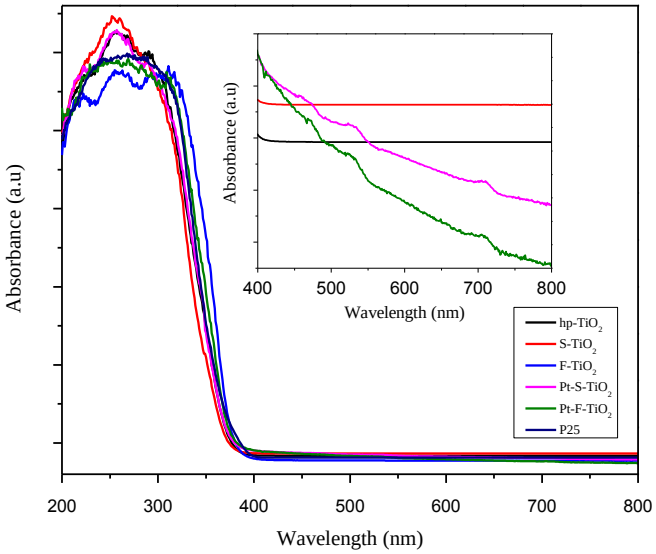

Figure 2. UV-Vis DR spectra for the photocatalysts analyzed.

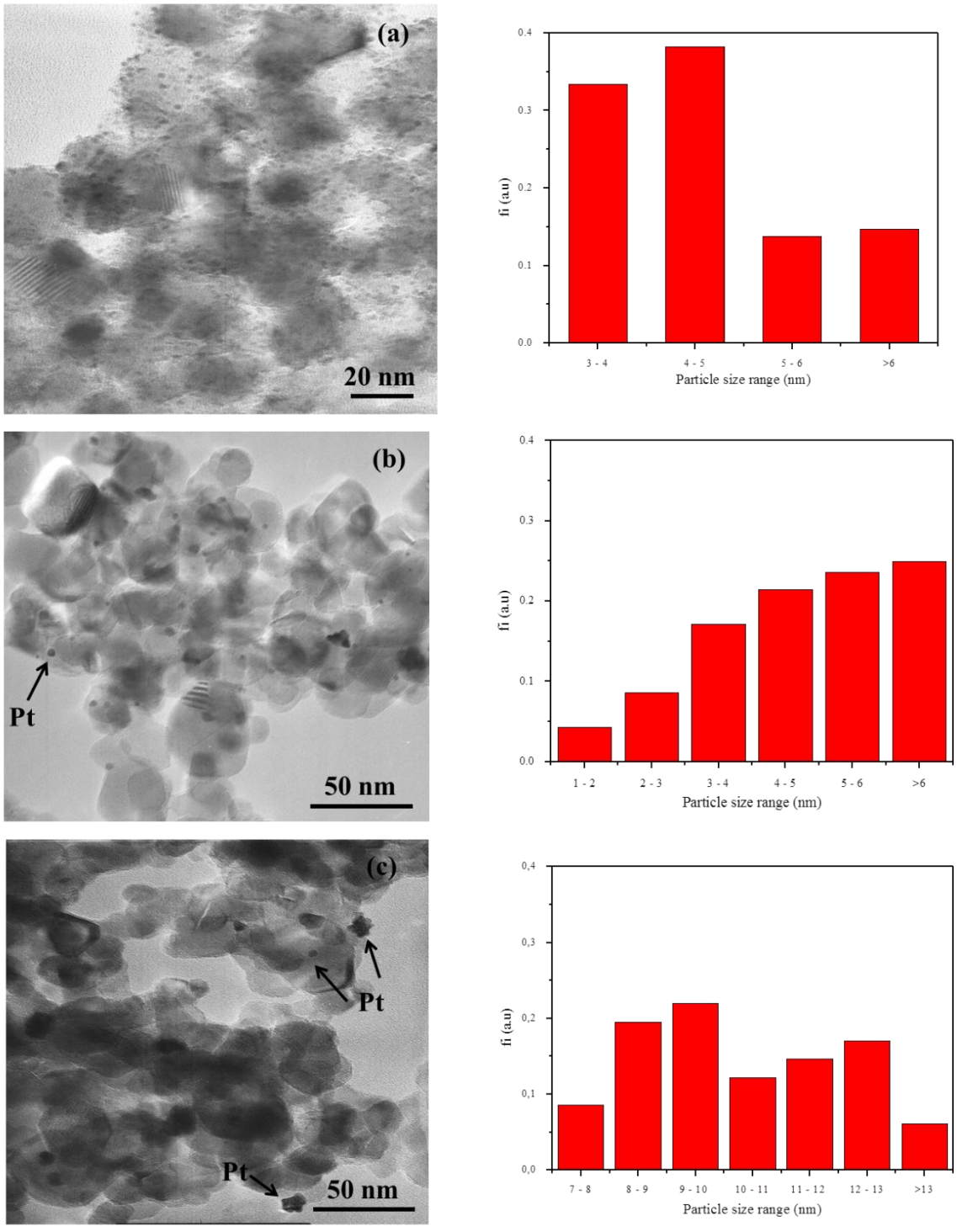

Figure 3. TEM images for analyzed samples. (a) Pt-S-TiO_2, (b) Pt-F-TiO_2 and (c) Pt-F-P25.

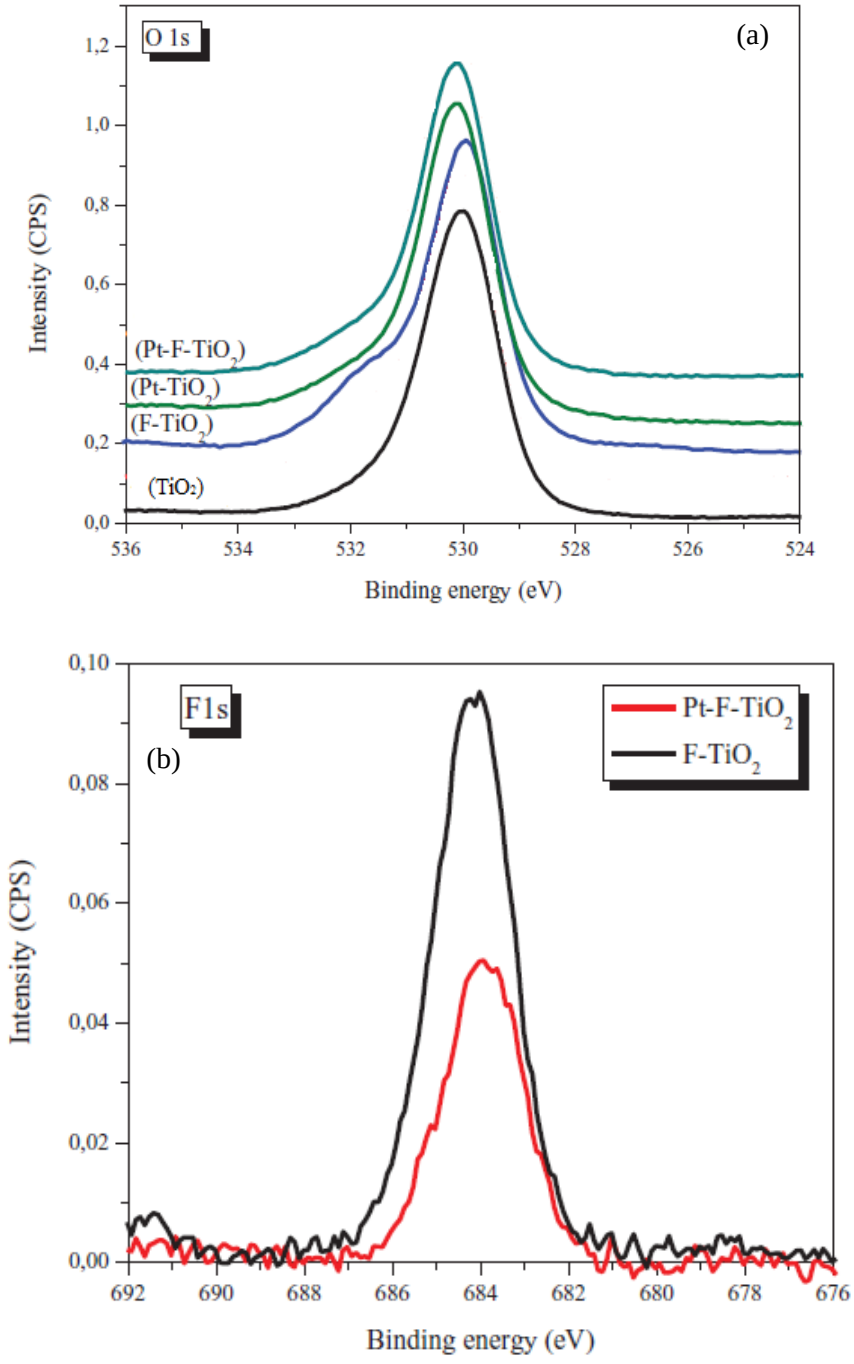

Figure 4. XPS core level spectra of O 1s and F 1s regions for selected samples.

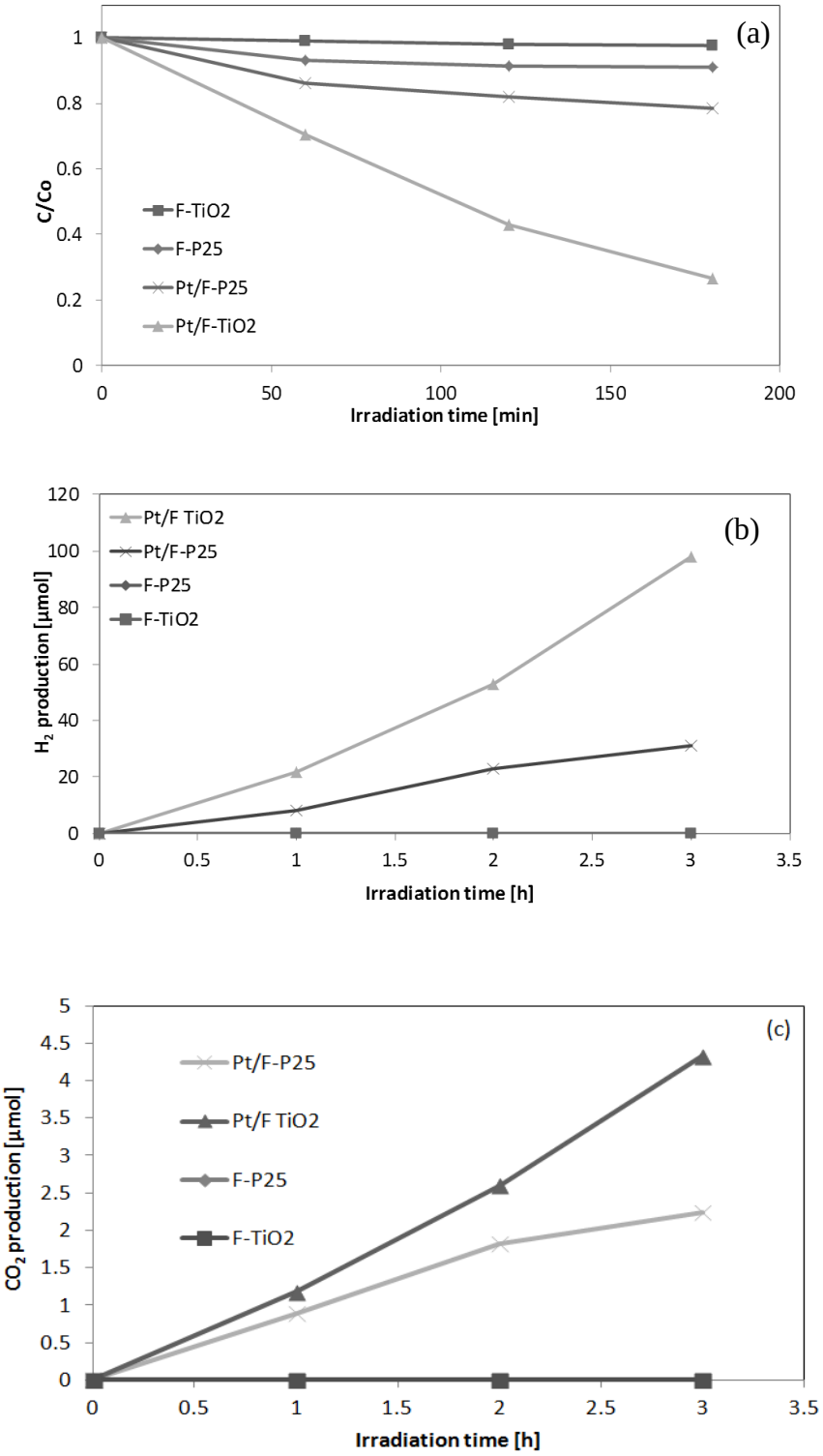

Figure 5. Behavior of glucose normalized concentration (a) H_2 (b) and CO_2 (c) production as a function of irradiation time; catalyst dose: 1.5 g/L; initial glucose concentration: 2000 mg/L; pH=6.

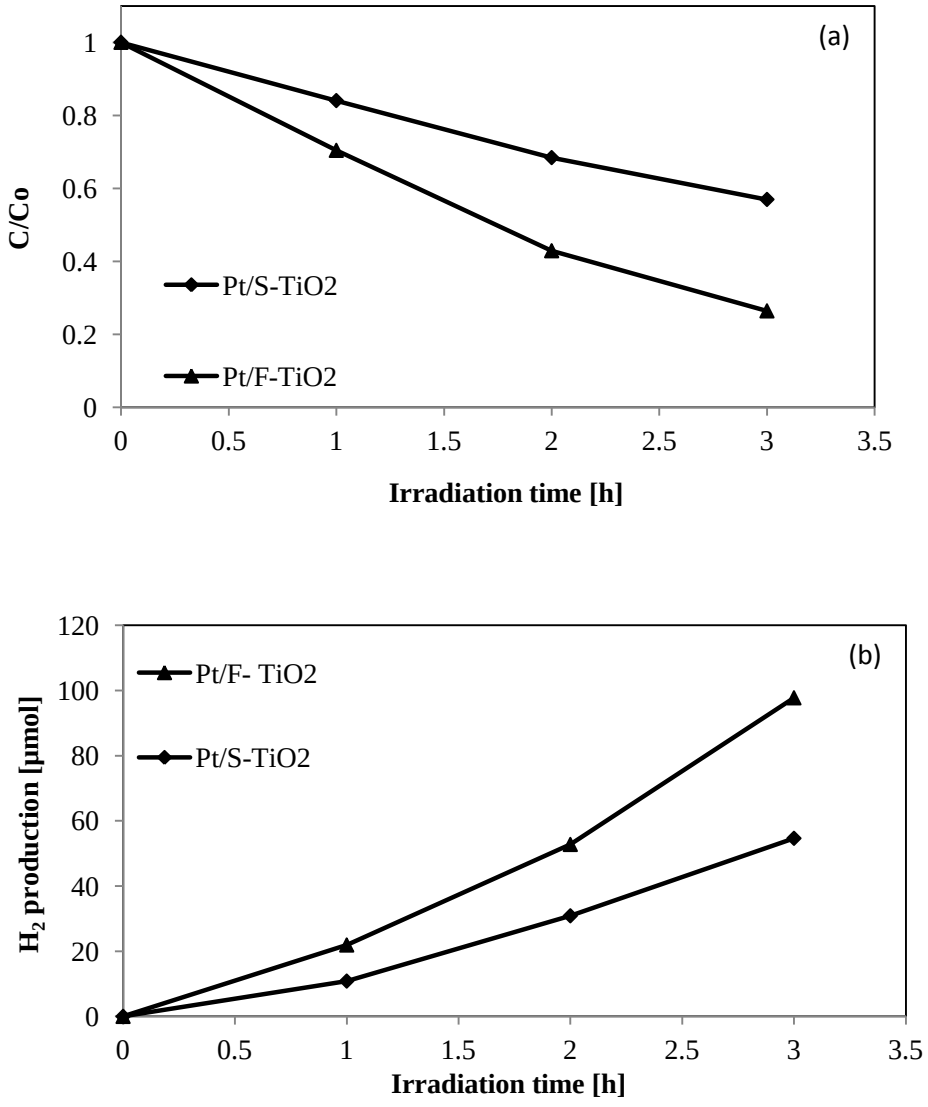

Figure 6. Behavior of glucose normalized concentration (a) and H_2 rate (b) during irradiation of fluorinated and sulfated TiO_2; catalyst dose: 1.5 g/L; initial glucose concentration: 2000 mg/L; pH=6.

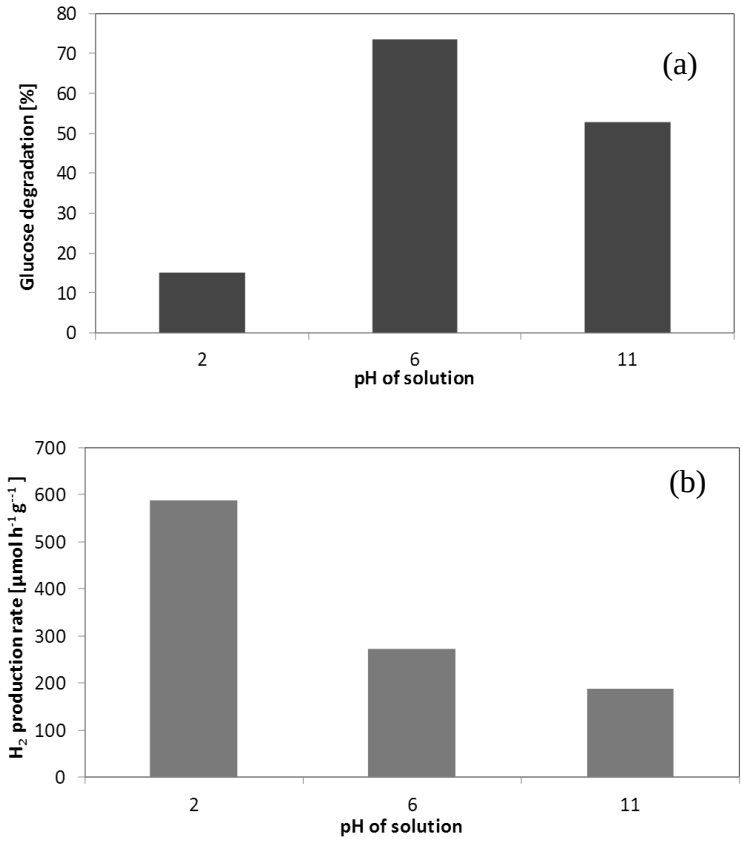

Figure 7. Effect of initial pH on glucose degradation (a) and H_2 production rate (b) for Pt-F-TiO_2 after 3 hours of irradiation; catalysts dose: 1.5 g/L; initial glucose concentration: 2000 mg/L.

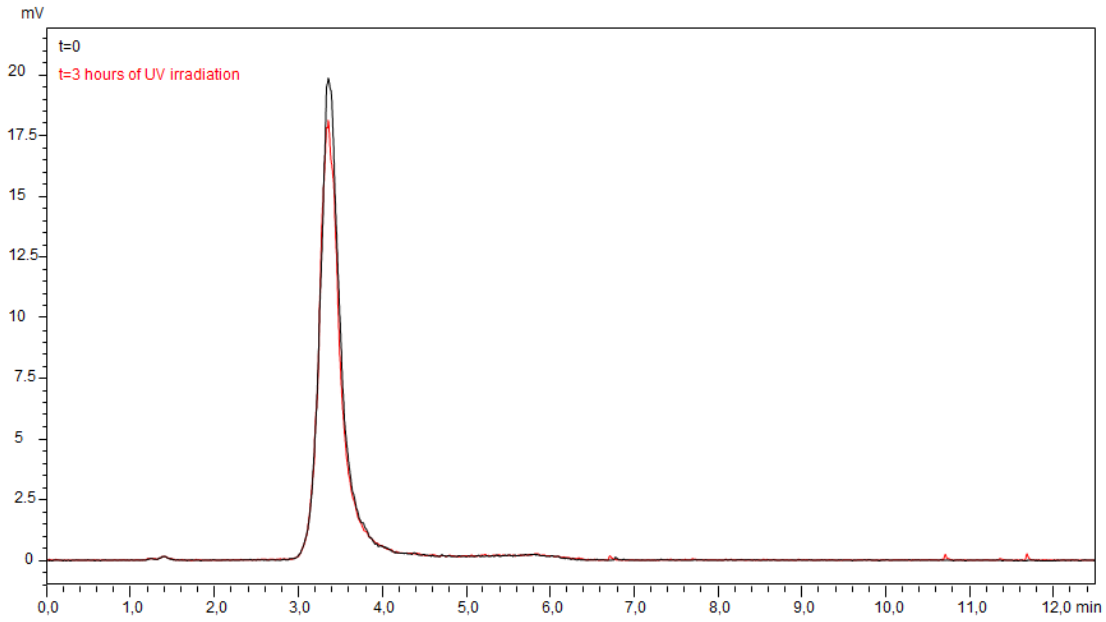

Figure 8. Typical HPLC chromatogram obtained during photocatalytic test on Pt-F-TiO_2 catalyst; initial glucose concentration : 2000 mg/L; initial pH =2.

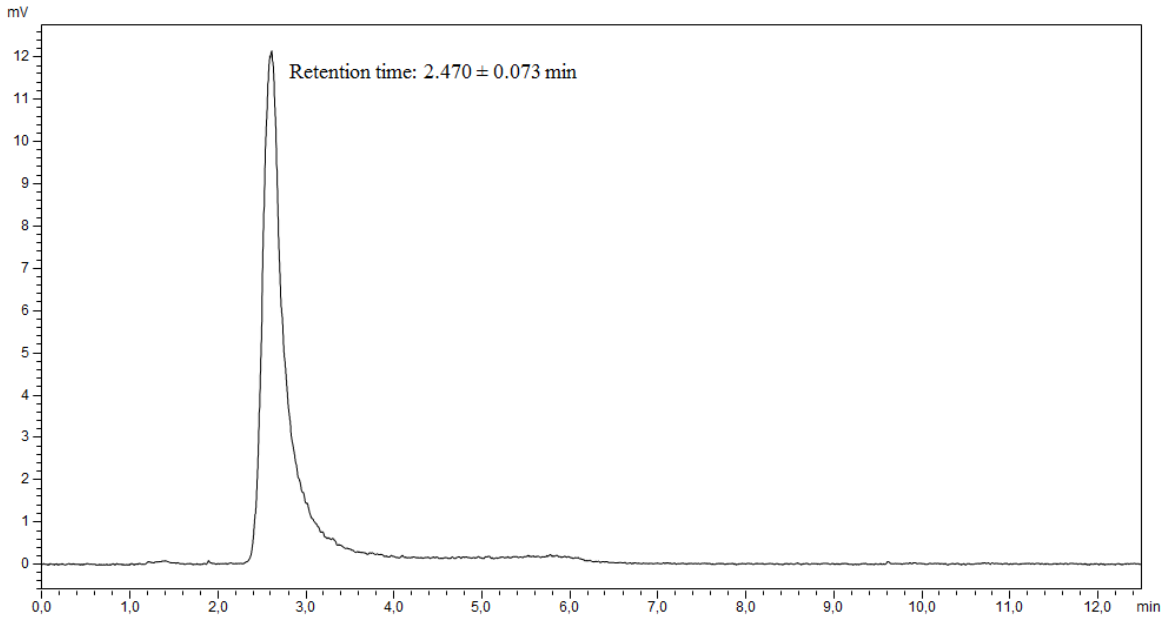

Figure 9. Typical HPLC chromatogram for a standard solution of arabinose.